

2023-08

# Spatial and Seasonal Variations in Dissolved Methane Across a Large Lake

Peacock, M

<https://pearl.plymouth.ac.uk/handle/10026.1/21714>

---

10.1029/2023jg007668

Journal of Geophysical Research: Biogeosciences

American Geophysical Union (AGU)

---

*All content in PEARL is protected by copyright law. Author manuscripts are made available in accordance with publisher policies. Please cite only the published version using the details provided on the item record or document. In the absence of an open licence (e.g. Creative Commons), permissions for further reuse of content should be sought from the publisher or author.*



## DATA ARTICLE

10.1029/2023JG007668

### Key Points:

- Lakes are globally important sources of atmospheric methane but there is a lack of data from large lakes >500 km<sup>2</sup>
- We measured methane concentrations across a large (1,074 km<sup>2</sup>) Swedish lake on five occasions over an annual period
- Methane varied seasonally and spatially, and higher concentrations were associated with nutrient inputs, lower dissolved oxygen, and shallower waters

### Supporting Information:

Supporting Information may be found in the online version of this article.

### Correspondence to:

M. Peacock,  
[m.peacock@liverpool.ac.uk](mailto:m.peacock@liverpool.ac.uk);  
[michael.peacock@slu.se](mailto:michael.peacock@slu.se)

### Citation:

Peacock, M., Davidson, S. J., Kothawala, D. N., Segersten, J., & Futter, M. N. (2023). Spatial and seasonal variations in dissolved methane across a large lake. *Journal of Geophysical Research: Biogeosciences*, 128, e2023JG007668. <https://doi.org/10.1029/2023JG007668>

Received 29 JUN 2023

Accepted 4 AUG 2023

© 2023. The Authors.

This is an open access article under the terms of the [Creative Commons Attribution License](https://creativecommons.org/licenses/by/4.0/), which permits use, distribution and reproduction in any medium, provided the original work is properly cited.

# Spatial and Seasonal Variations in Dissolved Methane Across a Large Lake

Mike Peacock<sup>1,2</sup> , Scott J. Davidson<sup>3</sup>, Dolly N. Kothawala<sup>4</sup>, Joel Segersten<sup>1</sup>, and Martyn N. Futter<sup>1</sup> 

<sup>1</sup>Department of Aquatic Sciences and Assessment, Swedish University of Agricultural Sciences, Uppsala, Sweden,

<sup>2</sup>Department of Geography and Planning, School of Environmental Sciences, University of Liverpool, Liverpool, UK,

<sup>3</sup>School of Geography, Earth and Environmental Sciences, University of Plymouth, Plymouth, UK, <sup>4</sup>Limnology/Department of Ecology and Genetics, Uppsala University, Uppsala, Sweden

**Abstract** Lakes process large volumes of organic carbon (OC), are important sources of methane (CH<sub>4</sub>), and contribute to climatic warming. However, there is a lack of data from large lakes >500 km<sup>2</sup>, which creates uncertainty in global budgets. In this data article, we present dissolved CH<sub>4</sub>, OC bioreactivity measurements, water chemistry, and algal biovolumes at 11 stations across Lake Mälaren, the third largest (1,074 km<sup>2</sup>) Swedish lake. Total phosphorus concentrations show that during the study period the lake was classed as mesotrophic/eutrophic. Overall mean CH<sub>4</sub> concentration from all stations, sampled five times to cover seasonal variation, was 2.51 μg l<sup>-1</sup> (0.98–5.39 μg l<sup>-1</sup>). There was no significant seasonal variation although ranges were greatest during summer. Concentrations of CH<sub>4</sub> were greatest in shallow waters close to anthropogenic nutrient sources, whilst deeper, central basins had lower concentrations. Methane correlated positively with measures of lake productivity (chlorophyll *a*, total phosphorus), and negatively to water depth and oxygen concentration, with oxygen emerging as the sole significant driver in a linear mixed effects model. We collated data from other lakes >500 km<sup>2</sup> (*n* = 21) and found a significant negative relationship between surface area and average CH<sub>4</sub> concentration. Large lakes remain an understudied contributor to the global CH<sub>4</sub> cycle and future research efforts should aim to quantify the spatial and temporal variation in their diffusive and ebullitive emissions, and associated drivers.

**Plain Language Summary** Lakes contribute to climatic warming, because they emit large amounts of the powerful greenhouse gas methane into the atmosphere. This occurs because lake bottom sediments and lake waters are home to microbes that produce methane, which then travels diffusively in a dissolved form, or as bubbles, through the lake water and into the air. There is large uncertainty about how much methane is released by lakes on a global scale, and more measurements are required to reduce this uncertainty, particularly from very large lakes. In our study, we measured dissolved methane from 11 sampling locations across a very large Swedish lake, and repeated this five times over a year. Levels of methane within the lake were generally low, but they varied over space and time. Higher methane levels occurred in shallower waters near large towns and cities, and were associated with greater concentrations of nutrients such as phosphorus, which act as food for the methane-producing microbes.

## 1. Introduction

Lakes emit globally relevant volumes of the potent greenhouse gas (GHG) methane (CH<sub>4</sub>) (Saunois et al., 2020) and therefore contribute to climatic warming. Total lake emissions have been estimated as ~100 Tg CH<sub>4</sub> yr<sup>-1</sup> (Bastviken et al., 2011) although there is considerable uncertainty in this figure, with recent estimates ranging 40–150 Tg CH<sub>4</sub> yr<sup>-1</sup> (Johnson et al., 2022; Lauerwald et al., 2023b; Rosentreter et al., 2021; Zheng et al., 2022). Synthesis studies show that small lakes have the largest emissions on an areal basis (i.e., per m<sup>2</sup> of lake surface), and the largest cumulative emissions (i.e., when all lakes are summed) (Holgerson & Raymond, 2016; Rosentreter et al., 2021). However, the majority of lake CH<sub>4</sub> research has focused on small lakes (<1 km<sup>2</sup>) and emissions from lakes >100 km<sup>2</sup> remain understudied (Deemer & Holgerson, 2021; Lauerwald et al., 2023a).

Emissions of CH<sub>4</sub> from lakes are generally positively correlated with measures of lake productivity such as nutrient (often phosphorus—P) and chlorophyll *a* concentrations (Bastviken et al., 2004; DelSontro et al., 2018), and temperature (Yvon-Durocher et al., 2014), because these increase the activity of CH<sub>4</sub>-producing methanogens (Segers, 1998). Thus, synergistic effects of climatic warming and eutrophication could further enhance lake CH<sub>4</sub>

**Table 1**  
Mean and Ranges in Surface CH<sub>4</sub> Concentrations for Other Large Lakes (>500 km<sup>2</sup>), Ordered by Surface Area

Lake	Country	Lake area (km <sup>2</sup> )	Average CH <sub>4</sub> (μg l <sup>-1</sup> )	CH <sub>4</sub> range (μg l <sup>-1</sup> )	Reference
Biwa	Japan	674	1.02	0.66–1.36	Miyajima et al. (1997)
Tumba	the DRC	694	1.06	not given	Borges et al. (2022)
St-Jean	Canada	1,065	0.14	0.08–0.19	DelSontro et al. (2018)
Mälaren	Sweden	1,074	2.51	0.98–5.39	This study
Champlain	Canada & US	1,269	1.42	1.01–2.34	DelSontro et al. (2018)
Vättern	Sweden	1,912	1.99	0.55–3.67	Pajala et al. unpublished
Mai Ndombe	the DRC	1,955	4.00	not given	Borges et al. (2022)
Edward	Uganda & the DRC	2,253	2.32	not given	Borges et al. (2022)
Taihu	China	2,338	2.47	0.22–7.68	Li et al. (2018)
Kivu	Rwanda & the DRC	2,371	0.99	not given	Borges et al. (2022)
Poyang	China	3,500	2.60	0.67–6.35	Wang et al. (2021)
Albert	Uganda & the DRC	5,402	1.17	not given	Borges et al. (2022)
Onega	Russia (European)	9,700	20.70	1.64–80.3	Gar'kusha and Fedorov (2015)
Ontario	Canada & US	19,009	0.51	0.22–0.69	DelSontro et al. (2018)
Winnipeg	Canada	23,750	0.67	0.08–11.7	Mandryk et al. (2021)
Erie	Canada & US	25,700	1.20	0.23–12.5	Fernandez et al. (2020)
Baikal	Russia (Asian)	31,722	0.08	0.01–66.4	Schmid et al. (2007)
Tanganyika	Tanzania, the DRC, Burundi, Zambia	32,821	0.30	not given	Borges et al. (2022)
Michigan	US	58,030	0.27	0.05–1.70	Joung et al. (2019)
Victoria	Kenya, Uganda, Tanzania	67,075	0.86	not given	Borges et al. (2022)
Superior	Canada & US	82,000	0.07	0.05–0.31	Joung et al. (2019)

Note. Average is mean, unless otherwise stated. Note that samples in Gar'kusha and Fedorov (2015) were collected from the shore only, most of which is under urban/industrial land cover. Overall mean = 2.2 μg l<sup>-1</sup>, or 1.3 μg l<sup>-1</sup> if the unusually high values from Gar'kusha and Fedorov (2015) are excluded. Spearman correlation shows a significant negative relationship between lake area and CH<sub>4</sub> concentration (rho = -0.46, p = 0.037).

emissions (Davidson et al., 2018) and create positive feedbacks to climate (Meerhoff et al., 2022). However, rising nutrient concentrations are not a certainty; many lakes, including some very large lakes, show declining P levels (Fink et al., 2018; Tong et al., 2017). Thus, there is a need to assess CH<sub>4</sub> dynamics in large lakes in order to reduce the uncertainty in global CH<sub>4</sub> budgets and provide baseline data for evaluating and tracking future changes.

Studies of CH<sub>4</sub> in large lakes (defined as having a surface area >500 km<sup>2</sup>, Herdendorf, 1982) have taken place in North America (Fernandez et al., 2020; Joung et al., 2019; Mandryk et al., 2021), Asia (L. Li et al., 2018; Liu et al., 2017; Miyajima et al., 1997; Schmid et al., 2007) and Africa (Borges et al., 2022; Roland et al., 2018) (Table 1). Studies in large European lakes are severely lacking and have often been process-focused; Sollberger et al. (2014) investigated benthic CH<sub>4</sub> dynamics in Lake Geneva whilst Hofmann et al. (2010) examined wave effects on littoral sediments and CH<sub>4</sub> release in Lake Constance. Gar'kusha and Fedorov (2015) measured shoreline CH<sub>4</sub> concentrations in one basin of Lake Onega in Russia (Gar'kusha & Fedorov, 2015) but shoreline measurements will likely overestimate CH<sub>4</sub> concentrations due to the proximity of anthropogenic nutrient point sources. Well-designed, temporally replicated, full lake surveys are needed to generate robust estimates of “what the atmosphere sees” (sensu Prairie et al., 2018).

Here, we measured dissolved CH<sub>4</sub> concentrations across 11 basins of a very large Swedish lake, with sampling repeated five times during different months to cover seasonal variation. Our study took place in conjunction with an established monitoring program, which provided a wealth of nutrient and algal data to place our measurements into context. We made additional laboratory measurements of dissolved organic carbon (OC) bioreactivity which, like CH<sub>4</sub>, is an understudied component of large lakes (Minor & Oyler, 2021). Our data set is likely to be a valuable resource for those researching biogeochemistry and phytoplankton in large lakes, and should provide guidance for those designing and planning GHG measurement campaigns in such waterbodies.

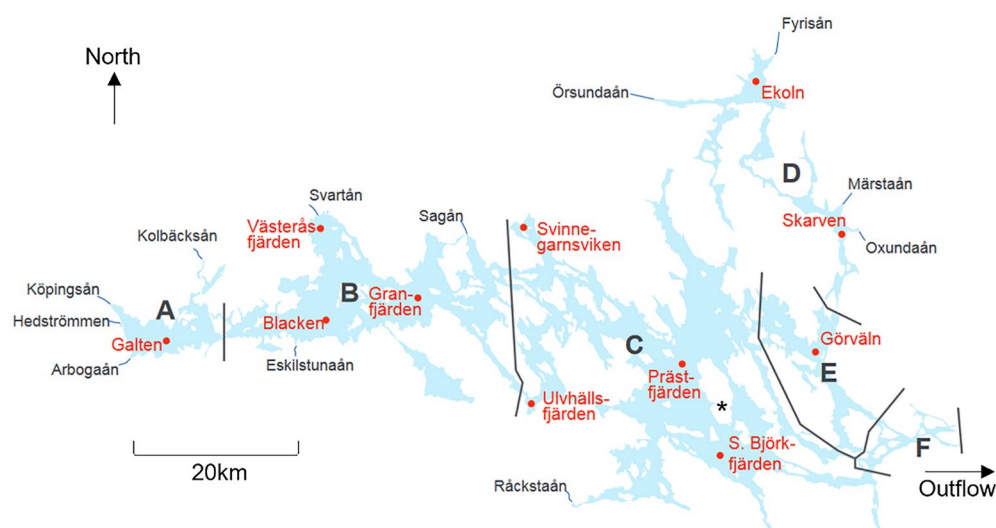


**Figure 1.** Map of Lake Mälaren, showing sampling points (red circles), lake basins (letters a–f, and demarcated by black lines), main rivers draining into Mälaren (blue lines, with river names in black), and location of the weather station (\*). Map is adapted from Sonesten et al. (2013).

## 2. Materials and Methods

### 2.1. Study Site

We collected samples from 11 locations across Mälaren (Figure 1) (59°24'N 17°24'E), on five separate occasions to cover seasonal variation: May, July, August and September 2019, and February 2020. Mälaren is the third largest Swedish lake and has a surface area of 1,074 km<sup>2</sup>, a volume of 14 km<sup>3</sup>, retention time of 2.8 years and mean and maximum depths of 12.8 and 66 m (SMHI, 2022a). Mälaren is dimictic (Johansson et al., 2010) and has a unique hydrogeomorphology and includes several interconnected basins with their own water residence times (Table 2). The shallowest waters are in the western basins (A and B) where several medium/large watercourses enter the lake, and the outlet is in the south-east at the capital city of Stockholm. Mälaren is in the hemiboreal vegetation zone (Sjors, 1999), and has a catchment of 22,620 km<sup>2</sup> which is predominantly forest (58%) agricultural land (19%), and lakes and watercourses (11%) (SMHI, 2022b). Urban land in the catchment is 3% and there are numerous cities and towns on, or within several kilometers of the lake shore. The climate is humid continental with a mean annual temperature (1st March 2019–29th February 2020) of 8.7°C, and total precipitation of 499 mm, both higher than long-term (1996–2021) means of 7.3°C and 468 mm (SMHI, 2022c). Winter temperatures are typically sub-zero, and the lake is usually ice covered for 1–5 months (SMHI, 2022d). The winter period (1st December 2019–29th February 2020) during our study was mild; mean daily temperatures were sub-zero on only 14 days, with the result that no long-term ice formed.

**Table 2**  
Areas, Volumes, Depths and Residence Times of the Individual Six Lake Basins

Basin	Area (km <sup>2</sup> )	Volume (km <sup>3</sup> )	Mean depth (m)	Max depth (m)	Residence time (years)
A	61	0.21	3.4	19	0.07
B	306	2.57	8.4	35	0.6
C	512	8.57	16.9	60	1.8
D	94	1.08	11.5	50	1.2
E	96	1.32	14	63	0.5
F	26	0.28	10.4	35	0.05

Note. Data from Sonesten et al. (2013). Note that no samples were collected from Basin F.

### 2.2. Sampling and Analysis

Samples for analysis of dissolved CH<sub>4</sub> concentration were made using the headspace technique, with one sample being collected at each location on each sampling occasion: 30 ml of surface water was taken in a 60 ml syringe directly from the lake, and then 30 ml of ambient air was also taken into the syringe. The syringe was then shaken for 1 min, which has been shown to be sufficient for efficient headspace CH<sub>4</sub> equilibrium (Roberts & Shiller, 2015). Whilst in the field, a sample of headspace gas was then injected into a pre-evacuated 12 ml glass Exetainer vial and returned to the lab, where CH<sub>4</sub> concentrations were measured using a Picarro GasScouter G4301 fitted with a sampling loop (Wilkinson et al., 2018). It has been suggested that some Exetainers may contain residual air that may introduce uncertainty into GHG

measurements (Sturm et al., 2015)—we made no adjustment for this possibility, but note that potential errors would be relatively low at the CH<sub>4</sub> concentrations in Lake Mälaren. Measurements of CH<sub>4</sub> in ppm were converted to dissolved concentrations using the solubility function of Wiesenburg and Guinasso (1979) and accounting for lake temperature and atmospheric pressure at the time of sampling, water:air volume in the syringe, and ambient air concentration (measured as 1.86 ppm by taking a sample of ambient air for analysis in an Exetainer). Atmospheric pressure data were taken from a weather station (SMHI, 2022c, see Figure 1). Flux measurements using floating chambers connected to the GasScouter may have been a preferable approach by allowing us to directly measure CH<sub>4</sub> emissions, but sampling logistics meant that we were limited to the quicker, simpler headspace sampling. Note that no analytical replicates of dissolved CH<sub>4</sub> concentration were taken; that is, only one Exetainer sample was taken for analysis at each sampling station on each occasion. Therefore, there is the possibility for some bias to enter our results due to sampling or analytical error.

Our CH<sub>4</sub> measurements took place within the framework of the research collaboration between the Swedish University of Agricultural Science (SLU) and Lake Mälaren's water conservation association (Mälarens vatten-  
vårdsförbund) (Drakare et al., 2021). At each site, measurements of water temperature, Secchi depth and dissolved oxygen (O<sub>2</sub>) were made in situ, and samples were taken for water chemistry analysis at SLU's SWEDAC-accredited Geochemical Laboratory for a wide variety of determinands: pH, alkalinity, electrical conductivity, turbidity, chlorophyll *a*, total organic carbon (TOC), total phosphorus (TP), total nitrogen, nitrite + nitrate, calcium, chloride, fluoride, potassium, magnesium, sodium, ammonium, silicon, sulfate, and filtered and unfiltered absorbance at 420 nm. All methods and any known issues are well-documented and are available online (SLU, 2022). During August and February additional sampling takes place at each station at depths throughout the water column to the lake bed; note that we refer to these measurements to put our results into context (see Drakare et al., 2021 for more detail). Within the same project framework, samples were collected for detailed measurements of phytoplankton at five stations (Ekoln, S. Björkfjärden, Granfjärden, Galten and Görväln) during May, July and September, and six stations during August (the aforementioned five stations, plus Blacken) (Drakare et al., 2021). We downloaded all water chemistry and phytoplankton data, which is freely available, for May, July, August and September 2019, and February 2020 (Miljödata-MVM, 2022a). For phytoplankton, we summed the biovolume of taxa within each of the following groups: Bacillariophyta, Charophyta, Chlorophyta, Choanoflagellida, Chrysophyceae, Cryptophyta, Cyanobacteria, Dinophyceae, Euglenophyceae, Haptophyta, Raphidophyceae, Synurophyceae, and “other phytoplankton”.

### 2.3. TOC Degradation Experiments

To investigate variations in TOC lability, we conducted laboratory incubation experiments. On each sampling occasion and at each station, a 500 ml sample of surface water was collected in a pre-rinsed 500 ml Nalgene bottle. Once returned to the lab, aliquots of each sample were measured for absorbance at 254 nm using a 1 cm path length cuvette and an Avantes AvaLight DH-S-BAL light source. Specific ultraviolet absorbance (SUVA), which provides information on the aromaticity of OC, was then calculated by normalizing absorbance at 254 nm by TOC concentration. Aliquots of all samples were then immediately transferred to 40 ml glass vials and placed in a WTW 1008-i thermostat cabinet at 20°C in the dark for 6 days. After this, samples were sent to the SLU Geochemical Laboratory for TOC analysis. Any changes in TOC concentration during incubations were therefore due to microbial activity (or physical processes such as flocculation) and represent short-term bioreactive OC (Soares et al., 2019).

### 2.4. Statistical Analysis

Trophic state was calculated for each station using mean annual TP concentrations: oligotrophic (TP < 12 µg l<sup>-1</sup>), mesotrophic (TP 12–24 µg l<sup>-1</sup>) and eutrophic (TP > 24 µg l<sup>-1</sup>) (IPCC, 2019). We calculated molar stoichiometric ratios for macronutrients: TOC:TP, TOC:TN, and TN:TP. Statistical analyses were first conducted in SPSS Statistics 26. Shapiro-Wilk tests showed that the total data set ( $n = 55$ ) of CH<sub>4</sub> measurements was non-normally distributed. Log10 transformations were used to normalize the data, before ANOVAs (with Tukey's HSD post-hoc tests) were used to test for differences in dissolved CH<sub>4</sub> concentration between sampling stations and sampling months. We used Spearman correlations, incorporating all data points, to test for relationships between dissolved CH<sub>4</sub>, OC bioreactivity, all water chemistry determinands, and algal biovolume. We then used a linear mixed effects (LME) model (R version 3.6.1 (R Core Team, 2013) with the nlme package (Pinheiro et al., 2018)), including all varia-

**Table 3**  
Sampling Station Locations, Plus Means and SEMs for CH<sub>4</sub> Concentration and Selected Water Quality Determinands, for All Five Sampling Months

Station	Location (lat, long)	Water depth (m)	CH <sub>4</sub> (μg l <sup>-1</sup> )	Chlorophyll (μg l <sup>-1</sup> )	NH <sub>4</sub> - N (μg l <sup>-1</sup> )	NO <sub>2</sub> + NO <sub>3</sub> - N (μg l <sup>-1</sup> )	pH	PO4-P (μg l <sup>-1</sup> )	Secchi depth (m)	O <sub>2</sub> (mg l <sup>-1</sup> )	TOC (mg l <sup>-1</sup> )	Tot-N (μg l <sup>-1</sup> )	Tot-P (μg l <sup>-1</sup> )	Turbidity (FNU)	EC (μS cm <sup>-1</sup> )	SUVA (l mg <sup>-1</sup> C <sup>-1</sup> m <sup>-1</sup> )	TOC loss (mg l <sup>-1</sup> )
Galten	59.446142, 16.187665	11	2.47 ± 0.59	16.4 ± 2.8	12.8 ± 4	148 ± 82	7.36 ± 0.07	6.8 ± 3.7	0.83 ± 0.12	11.18 ± 0.69	10.7 ± 1.1	644 ± 106	46.9 ± 7.4	20.2 ± 6.2	142 ± 3	3.06 ± 0.4	0.7 ± 0.4
Västeråsfjärden	59.592772, 16.552613	10	4.43 ± 0.32	13 ± 3.5	23.2 ± 5	379 ± 125	7.57 ± 0.1	7.2 ± 4.3	1.11 ± 0.18	11.52 ± 0.79	10 ± 1	865 ± 150	41.3 ± 7.5	12.9 ± 3.8	386 ± 5	2.92 ± 0.4	0.42 ± 0.3
Blacken	59.473605, 16.544335	30	2.45 ± 0.24	9 ± 1.8	13.8 ± 3.2	378 ± 67	7.52 ± 0.05	5.8 ± 3.1	1.41 ± 0.21	11.44 ± 0.85	9.5 ± 0.7	810 ± 80	31.4 ± 4.8	9.9 ± 3	109 ± 6	2.59 ± 0.6	0.36 ± 0.3
Granfjärden	59.494454, 16.810836	36	2.28 ± 0.38	7.2 ± 1.4	17.8 ± 6.3	286 ± 74	7.64 ± 0.09	6.4 ± 3.8	1.61 ± 0.21	11.47 ± 0.9	8.9 ± 0.6	701 ± 79	30.8 ± 6.1	8.8 ± 3.2	231 ± 4	2.88 ± 0.4	0.2 ± 0.3
Svinmegarnsviken	59.581140, 17.045103	10	3.33 ± 0.39	9.5 ± 2.4	15.4 ± 3.6	227 ± 131	7.74 ± 0.13	6.8 ± 5	1.31 ± 0.19	11.46 ± 0.42	8.4 ± 0.4	655 ± 127	29 ± 6.1	8.2 ± 3.1	152 ± 3	3.15 ± 0.6	0.34 ± 0.2
Ulvhällsfjärden	59.367831, 17.055091	9	3.05 ± 0.41	12.8 ± 3	34.6 ± 11.6	148 ± 85	7.64 ± 0.04	4.4 ± 3.5	1.51 ± 0.17	11.46 ± 0.76	8.7 ± 0.4	632 ± 77	32.4 ± 3.1	7.3 ± 1.8	174 ± 1	2.6 ± 0.2	0.48 ± 0.3
Prästfjärden	59.426957, 17.426581	50	1.29 ± 0.1	5.1 ± 1.1	8.2 ± 1.4	60 ± 37	8.02 ± 0.17	4.6 ± 3.5	3.36 ± 0.12	12.02 ± 0.86	7.4 ± 0.1	436 ± 25	16.8 ± 2.6	1.8 ± 0.5	396 ± 1	2.72 ± 0.5	0.26 ± 0.2
Södra Björkfjärden	59.290190, 17.519937	44	1.43 ± 0.13	4.2 ± 0.8	14.2 ± 4.4	49 ± 32	8.02 ± 0.14	4.2 ± 3.5	3.5 ± 0.24	12.03 ± 0.96	7.3 ± 0.1	424 ± 23	15.6 ± 2.6	1.6 ± 0.3	173 ± 1	2.94 ± 0.2	0.18 ± 0.2
Ekoln	59.751114, 17.608240	30	2.38 ± 0.36	13.2 ± 3.9	11.2 ± 3	1,116 ± 145	8.04 ± 0.08	8.4 ± 5.9	1.99 ± 0.37	11.52 ± 0.8	13.3 ± 0.8	1744 ± 165	35.9 ± 7.5	5.5 ± 2.8	178 ± 4	2.61 ± 0.1	0.68 ± 0.1
Skarven	59.553666, 17.807456	30	2.42 ± 0.31	10.3 ± 2.1	13.2 ± 2.9	551 ± 178	8.17 ± 0.11	6 ± 5.4	2.38 ± 0.35	11.7 ± 1.06	11.7 ± 0.4	1132 ± 153	27.3 ± 4.5	3.1 ± 1.2	158 ± 2	2.82 ± 0.3	0.4 ± 0.3
Görvåln	59.419460, 17.739984	48	2.1 ± 0.16	7.8 ± 2.3	7.2 ± 0.9	59 ± 47	8.13 ± 0.13	3.2 ± 2.9	2.92 ± 0.18	12.17 ± 0.86	8.2 ± 0.1	493 ± 38	17.4 ± 2.4	1.6 ± 0.4	152 ± 3	3.0 ± 0.7	0.44 ± 0.4

Note. Stations are ordered approximately west to east across the lake (i.e., the direction of water flow).

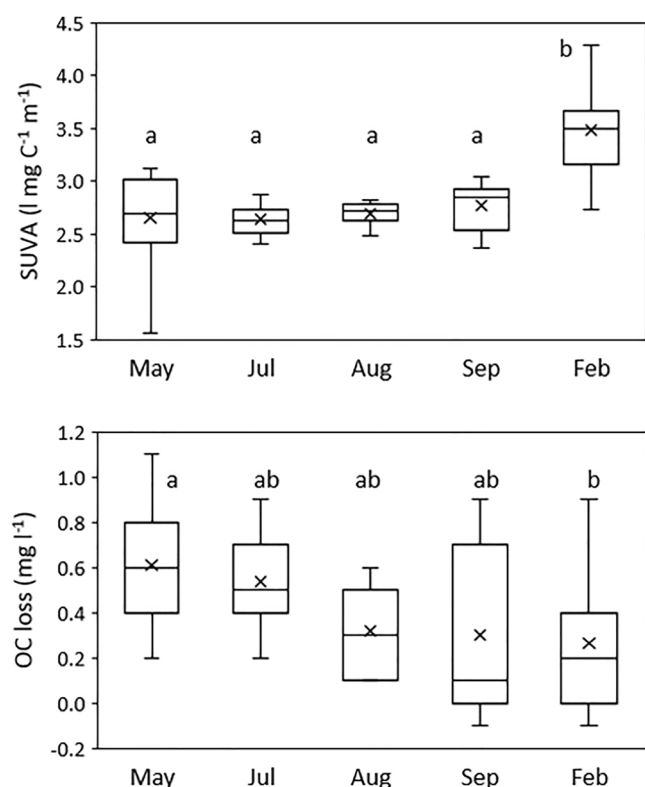


**Figure 2.** Box plots of Specific ultraviolet absorbance (SUVA) and short-term bioreactive organic carbon (OC) for all five sampling months for each sampling station. Boxes represent medians and interquartile range (IQR), whiskers mark minimum and maximum values. Also shown are mean concentrations ( $x$ ). There are no outliers. ANOVA shows significant differences for SUVA ( $F = 14.0$ ,  $p < 0.001$ ) and bioreactive OC ( $F = 3.75$ ,  $p = 0.01$ ) between months; months with shared letters indicate no significant differences.

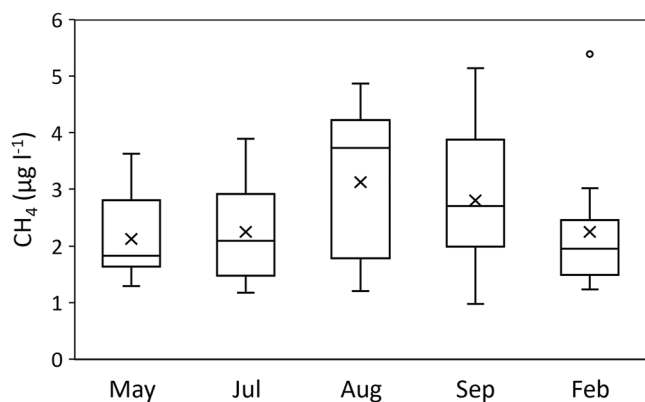


**Figure 3.** Box plot of  $\text{CH}_4$  concentrations from all 11 sampling stations for each sampling month. Boxes represent medians and interquartile range (IQR), whiskers mark minimum and maximum values, excluding outliers (calculated as box limits  $\pm 1.5 \times \text{IQR}$ ). Also shown are means ( $x$ ) and outliers ( $o$ ). ANOVA shows no significant difference between months.

bles that were significantly correlated with  $\text{CH}_4$  in the Spearman correlations (with the exception of water depth as this was considered unchanging at each station throughout the study, and phytoplankton which wasn't measured at all stations and dates). Site was included as a random effect. We calculated the amount of variance described by the model as  $R^2_{\text{GLMM}}$  (Nakagawa & Schielzeth, 2013), using the package MuMIn (Bartoń, 2019). Results for all tests were considered significant if  $p < 0.05$ , and nominal  $p$  values are presented throughout. Errors are given as standard error of the means.

### 3. Results and Discussion

#### 3.1. Lake Biogeochemistry and OC Bioreactivity

Measured TP concentrations showed that the lake's trophic state was mesotrophic/eutrophic: the stations Görvälän, Prästfjärden and S. Björkfjärden were mesotrophic, whilst all other stations were eutrophic (Table 3). For all 11 stations and months there was a clear seasonality to surface water temperature through May, July, August, September 2019, and February 2020, with respective means of 14.2, 17.7, 20.0, 14.8, and 2.3°C. For all stations and seasons, mean SUVA was 2.85 (range 1.56–4.28)  $\text{l mg C}^{-1} \text{m}^{-1}$ , suggesting a low/medium degree of OC aromaticity (Weishaar et al., 2003). SUVA values from the Laurentian Great Lakes are  $\sim 1.2 \text{ l mg C}^{-1} \text{m}^{-1}$  (Zhou et al., 2016). These lakes are an order of magnitude larger than Mälaren, and thus the higher SUVA values we report likely indicate greater terrestrial OC inputs. Bioreactivity experiments showed that over 6 days the mean change in OC was 0.4 (range  $-0.1$ – $1.1$ )  $\text{mg l}^{-1}$ . There is a lack of comparable data (Minor & Oyler, 2021), but others have found that OC in large lakes can be bioavailable over short time periods (Laird & Scavia, 1990). Our OC losses are greater than those reported for Swedish rivers by Soares et al. (2019) who also measured over 6 days, with a mean loss of 0.17  $\text{mg l}^{-1}$ . The difference may be due to trophic state; their sites had lower TP concentrations and were predominantly mesotrophic, and they found that greater nutrient inputs stimulated primary production and therefore increased short-term OC losses. Our results agree with this interpretation; a significant correlation was found between OC bioreactivity and chlorophyll  $a$  ( $\rho = 0.37$ ,  $p = 0.005$ , Figure S1 in Supporting Information S1). For seasonal variation SUVA was significantly ( $F = 14.0$ ,  $p < 0.001$ ) higher during February (mean 3.48  $\text{l mg C}^{-1} \text{m}^{-1}$ ) than all other months (mean = 2.7  $\text{l mg C}^{-1} \text{m}^{-1}$ ) (Figure 2). The only significant difference for OC loss was between February and May (respective means of 0.26 and 0.6  $\text{mg l}^{-1}$ ,  $p = 0.03$ ). ANOVAs showed no significant differences in SUVA ( $F = 0.93$ ,  $p = 0.5$ ) or OC loss ( $F = 2.0$ ,  $p = 0.06$ ) between sites (Figure 2).

#### 3.2. Spatial and Seasonal Variations in $\text{CH}_4$

Overall mean dissolved  $\text{CH}_4$  for the study was  $2.51 \pm 0.15 \text{ } \mu\text{g l}^{-1}$ , range 0.98–5.39  $\mu\text{g l}^{-1}$ , which is similar to mean concentrations in other large lakes (overall mean = 1.41  $\mu\text{g l}^{-1}$ , Table 1), including unpublished measurements from Vättern, Sweden's second largest lake (1,900  $\text{km}^2$  surface area, mean depth of 41 m) where 4 years of summer/autumn headspace measurements gave a mean of 1.99  $\mu\text{g l}^{-1}$ , range 0.55–3.67  $\mu\text{g l}^{-1}$  (Pajala et al., unpublished). No significant differences were found between the five sampling campaigns ( $F = 1.35$ ,  $p = 0.26$ ), although there was a clear seasonal pattern whereby means and ranges of  $\text{CH}_4$  concentrations were greatest during the end of summer (August and September) (Figure 3), with a mean of

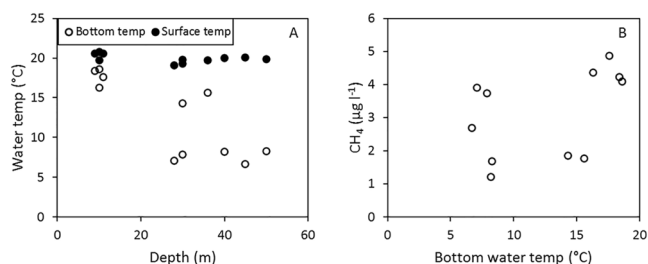


**Figure 4.** Panel (a) scatter plot showing water temperatures as a function of lake depth for the 11 sampling stations during August. Water temperatures are shown at the lake surface (filled circles) and in bottom waters (open circles). There is a significant correlation ( $\rho = -0.7, p = 0.016$ ) between depth and bottom water temperature. Panel (b) scatter plot of surface  $\text{CH}_4$  concentration and bottom water temperature for the 11 sampling stations during August. The correlation is not significant ( $\rho = 0.45, p = 0.16$ ).

$3.13 \pm 0.38 \mu\text{g l}^{-1}$  for the whole lake in August when mean water temperature peaked. The lack of seasonality could be due to deep waters remaining thermally stratified, with the result that lake sediments are buffered from air temperature variations, and so deep-water sediments remain cold year-round, with no summer increase in methanogenesis rates. Monitoring data supports this (Figure 4a) and shows a clear disconnect between surface water and bottom water temperatures at the deep water stations; during our August sampling, surface water temperature at the station with deepest water (Prästfjärden) was  $19.9^\circ\text{C}$ , whilst at 50 m depth the temperature was  $8.3^\circ\text{C}$ . At the shallowest station (Ulvhällsfjärden) during August surface water was  $20.6^\circ\text{C}$  and the deepest waters (9 m) were  $18.4^\circ\text{C}$ . Thus, at the stations with shallow waters the sediments will be warmer during summer, favoring seasonal increases in  $\text{CH}_4$  production and we note that others have shown that bottom water temperatures in very large lakes do relate to surface  $\text{CH}_4$  emissions (Fernandez et al., 2020; Liu et al., 2017). However, although shallower, warmer stations tended toward higher summertime  $\text{CH}_4$ , there was not

a significant correlation between bottom water temperature and  $\text{CH}_4$  (Figure 4b) suggesting that other drivers are also involved.

Significant differences in  $\text{CH}_4$  concentrations were found spatially between sampling stations (Figure 5, Table 3) with the highest mean concentrations in Västeråsfjärden ( $4.43 \pm 0.32 \mu\text{g l}^{-1}$ ), Svinnegarnsviken ( $3.33 \pm 0.39 \mu\text{g l}^{-1}$ ) and Ulvhällsfjärden ( $3.05 \pm 0.41 \mu\text{g l}^{-1}$ ). These three stations are all located in shallow bays or straits (depth  $\leq 10$  m) that are close to towns/cities with relatively large populations (respective populations of  $\sim 130,000, 30,000,$  and  $15,000$ ), and the waters are thus subject to anthropogenic nutrient inputs and particulate matter settling into the sediment. Although we did not track nutrient inputs into the lake, other research has shown high concentrations of organic micropollutants (including pharmaceuticals, industrial chemicals, pesticides, etc), particularly at sampling stations near to large towns and cities (Rehrl et al., 2020) demonstrating an anthropogenic influence on lake water quality. In contrast to this, lowest mean  $\text{CH}_4$  concentrations were at stations in the center of the deep (44–50 m) basin C (Figure 5, Table 3, Prästfjärden,  $1.29 \pm 0.10 \mu\text{g l}^{-1}$ , and S. Björkfjärden,  $1.43 \pm 0.13 \mu\text{g l}^{-1}$ ) where nutrient concentrations were also lower; total P and chlorophyll *a* concentrations were approximately half of their values at the three high- $\text{CH}_4$  stations (Table 3): overall means of 16.2 versus  $34.2 \mu\text{g l}^{-1}$  total P, and 4.65 versus  $11.8 \mu\text{g l}^{-1}$  for chlorophyll *a*.

Mean  $\text{CH}_4$  was low during February 2020 ( $2.25 \mu\text{g l}^{-1} \pm 0.34$ ), and the variation in  $\text{CH}_4$  across the whole lake was also smallest at this point. However, a clear outlier occurred at this time, with the shallow-water Västeråsfjärden

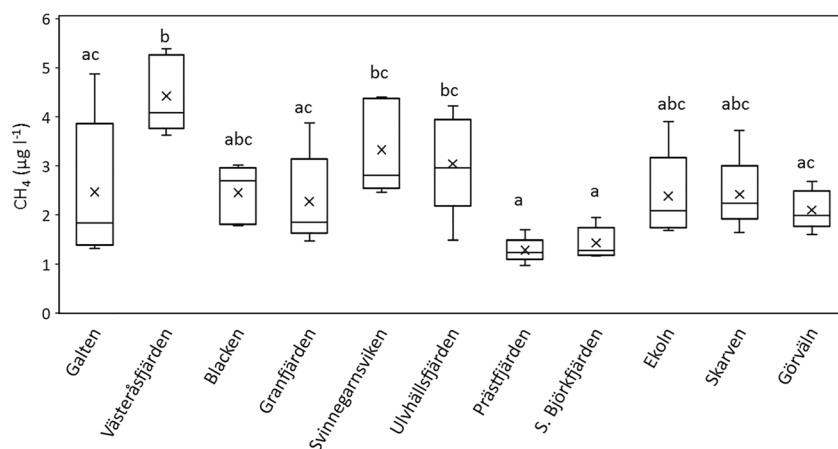


**Figure 5.** Box plot of  $\text{CH}_4$  concentrations for all five sampling months for each sampling station. Stations are ordered approximately west to east across the lake (i.e., the direction of water flow). Boxes represent medians and interquartile range (IQR), whiskers mark minimum and maximum values. Also shown are mean concentrations (x). There are no outliers. ANOVA shows significant differences ( $F = 6.07, p < 0.001$ ) between stations; stations with shared letters indicate no significant differences.



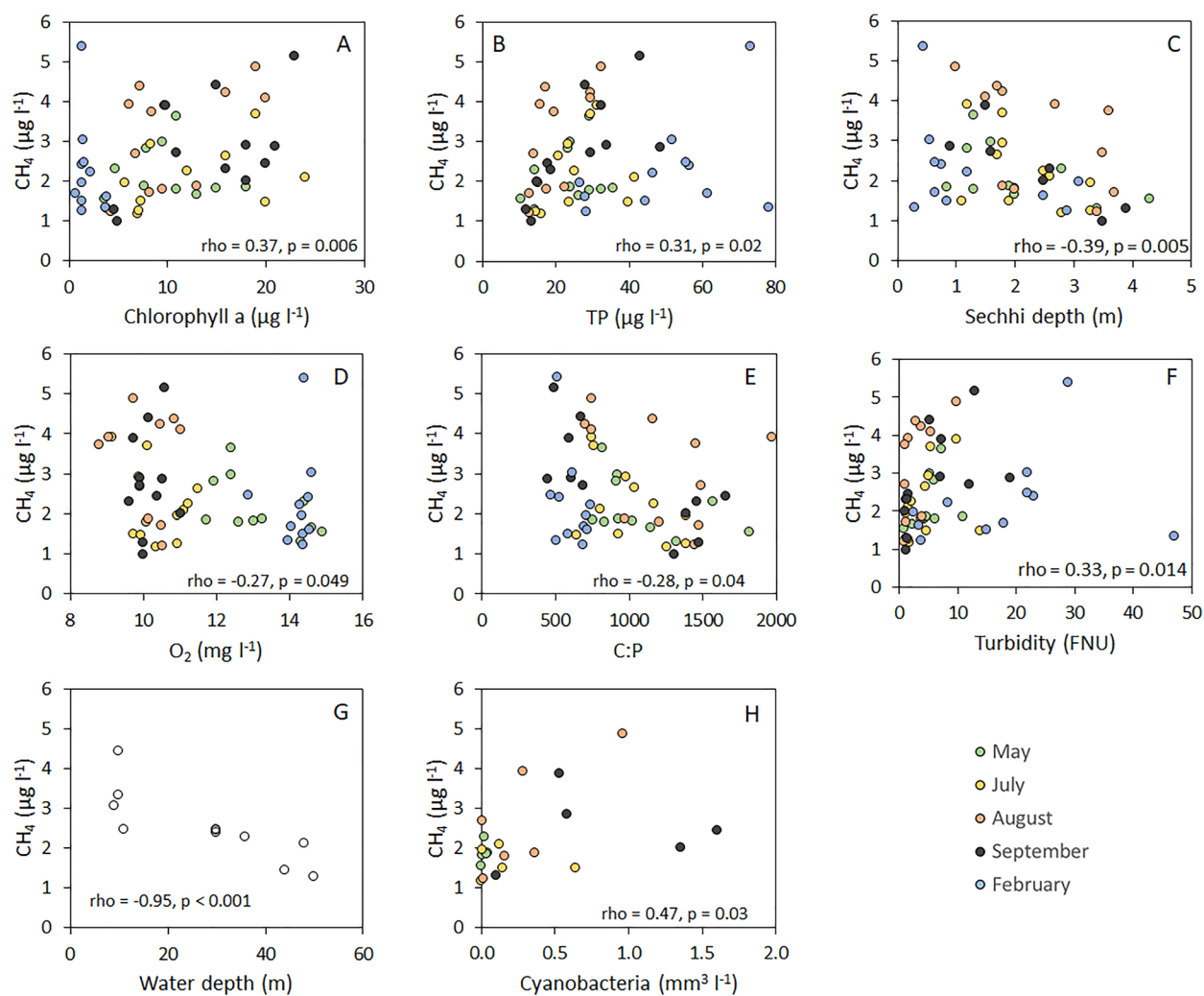


**Figure 6.** Scatter plots showing relationships between CH<sub>4</sub> concentrations and: chlorophyll *a* concentrations (a), total phosphorus concentration (b), Sechhi depth (c), oxygen concentration (d), the molar stoichiometric ratio of organic carbon to phosphorus (e), turbidity (f), water depth (g) and Cyanobacteria biovolume (h).

station having the highest CH<sub>4</sub> concentration measured during the entire study (5.39 μg l<sup>-1</sup>) (Figure 3). This was despite cold temperatures (mean surface water 2.3°C) which would be expected to decrease CH<sub>4</sub> production rates (Fernandez et al., 2020; Liu et al., 2017). Without analytical replicates (see Section 2.2) we cannot fully eliminate the possibility that this value relates to analytical or sampling error. Assuming it is real, one possibility is that this anomaly could arise following several days of low wind speeds, whereby a decrease in piston velocity might lead to an increase in water column CH<sub>4</sub> concentrations—this hypothesis can be dismissed, because wind speeds during the study period were highest at the start of 2020, with monthly means of 4.2 m s<sup>-1</sup> for January and February (SMHI, 2022c). Another, more plausible hypothesis involves rain: at the start of 2020, high volumes of precipitation fell on bare ground, which was free of snow and ice due to unusually mild winter temperatures. Within the Mälaren catchment, high flows are positively related to turbidity and TOC (Lannergård et al., 2021; LeDesma et al., 2012), and therefore this winter rain event led to elevated levels of both within some of the rivers entering the lake (Drakare et al., 2021). These increased terrestrial inputs are also evident in the significantly higher SUVA values during February (Figure 2). In turn, this led to unusually high increases in TP concentrations, because phosphorus transport within the catchment is largely driven by particle-associated P from agricultural clay soils (Lannergård et al., 2019), and the mobilization of these particles can be particularly high during winter when riparian vegetation is absent (Lannergård et al., 2021). Upon entering the lake, riverine particulates will settle out, thus delivering additional P to bottom sediments. TP and TOC were particularly high at Västeråsfjärden in February, reaching 73.1 μg l<sup>-1</sup> and 14.6 mg l<sup>-1</sup>, respectively 149% and 54% higher than overall means for those

measures. Assuming that these high water column P and C concentrations translate into elevated nutrient levels in sediments, then CH<sub>4</sub> production will be enhanced (Bastviken et al., 2004; Deemer & Holgerson, 2021) despite low temperatures (Juutinen et al., 2009), although additional samples or lab incubations would be necessary to confirm this suggestion. Intriguingly, another station (Galten) had even higher concentrations of TP and TOC during February (78 μg l<sup>-1</sup> and 15.4 mg l<sup>-1</sup>, respectively) but CH<sub>4</sub> remained low, at 1.32 μg l<sup>-1</sup>. The difference between CH<sub>4</sub> responses to high nutrient loads at this time may be due to residence times; Västeråsfjärden's basin has a residence time of 0.6 years whilst Galten's is 0.07 years. Thus, the nutrient inputs to Galten could have been rapidly fluxed through the basin and on into deeper lake waters, with the result that no in situ sedimentary CH<sub>4</sub> hotspot developed.

### 3.3. Drivers of CH<sub>4</sub> Variation

There were no significant Spearman correlations between CH<sub>4</sub> and surface water temperature ( $\rho = 0.2$ ,  $p = 0.15$ ) in line with statistical tests highlighting a lack of seasonality (Section 3.2). Observations that nutrient status and water depth were important drivers of CH<sub>4</sub> concentrations (Section 3.2) were supported by correlations which showed significant positive relationships between CH<sub>4</sub> and chlorophyll *a*, and CH<sub>4</sub> and TP, and negative relationships between CH<sub>4</sub> and station depth, O<sub>2</sub>, turbidity, Secchi depth, and C:P (Figures 6a–6g). The LME model, developed using these significant Spearman correlations (with the exception of station depth which was assumed constant at each station), detected a significant relationship between O<sub>2</sub> and CH<sub>4</sub> ( $F_{1,34} = 5.4$ ,  $p = 0.026$ ) but no significant relationships between CH<sub>4</sub> and Chlorophyll *a* ( $F_{1,34} = 1.5$ ,  $p = 0.25$ ), Secchi depth ( $F_{1,34} = 1.9$ ,  $p = 0.18$ ), TP ( $F_{1,34} = 0.03$ ,  $p = 0.87$ ), turbidity ( $F_{1,34} = 7.9$ ,  $p = 0.38$ ) or C:P ( $F_{1,34} = 0.98$ ,  $p = 0.32$ ). The model explained 38% of the variance. The difference in significant variables between the Spearman correlations and LME model is likely due to confounded variables. Thus, some correlations should not be used to infer mechanistic relationships with CH<sub>4</sub>; for example, there were strong relationships between Secchi depth and turbidity ( $\rho = -0.95$ ,  $p < 0.001$ ), and between TP and turbidity ( $\rho = 0.89$ ,  $p < 0.001$ ) (Figure S2 in Supporting Information S1). Thus, we assume that TP controls CH<sub>4</sub> dynamics (Bastviken et al., 2004; DelSontro et al., 2016) and, because much of this TP is associated with particles (Lannergård et al., 2019), Secchi depth and turbidity are also correlated. Greater TP concentrations will result in high-chlorophyll *a*, low-O<sub>2</sub>, eutrophic conditions (DelSontro et al., 2018), with higher rates of methanogenesis in sediments (West et al., 2016). The negative correlation between CH<sub>4</sub> and C:P (Figure 6e) shows that more C relative to P leads to lower CH<sub>4</sub>, and has been reported in reservoirs (Z. Li et al., 2020). This finding agrees with a growing body of work arguing that nutrient stoichiometry, and not just absolute concentration, is important in controlling aquatic biogeochemistry (Graeber et al., 2021; Peacock et al., 2022; Stutter et al., 2018; Taylor & Townsend, 2010), including GHG emissions (Peacock et al., 2017; Webb et al., 2021). Finally, a negative relationship between surface water CH<sub>4</sub> concentration and water depth (Figure 6g) is frequently reported (Deemer & Holgerson, 2021; Juutinen et al., 2009; Natchimuthu et al., 2016) and is likely due to a greater opportunity for methanotrophy within the water column of deeper lakes (M. Li et al., 2020), as well as colder sediments having lower rates of methane production (Schulz et al., 1997). However, we emphasize again that many of these correlations could be confounded, making interpretations difficult. For instance, mean annual TP and station depth were also strongly negatively correlated ( $\rho = -0.71$ ,  $p = 0.014$ , Figure S3 in Supporting Information S1). In part this is likely due to the fact that fluvial nutrient loads discharge into shallow basins (Section 3.2), but sediment P resuspension will also be greater in shallow waters (Reddy et al., 1996). Thus, it becomes somewhat unclear whether TP controls CH<sub>4</sub>, or whether TP and CH<sub>4</sub> are both controlled by depth; the lack of a direct correlation between sediment temperature and CH<sub>4</sub> (Section 3.2) points perhaps to a combined role of depth (via methanotrophy in the water column) and TP. Our theorizing of how depth affects surface CH<sub>4</sub> concentrations rests on the assumption that CH<sub>4</sub> production is primarily occurring in sediments. However, there is the possibility that CH<sub>4</sub> production is also taking place within the oxygenated water column (Bogard et al., 2014; Grossart et al., 2011). Our data offer an intriguing hint that this may be occurring. For the subset of sites and months where algal data were available (for 13 algal groups), the only significant algal relationship with CH<sub>4</sub> was a positive correlation with Cyanobacteria biovolume (Figure 6h). Unlike CH<sub>4</sub> concentration, cyanobacteria biovolume showed a clear seasonal trend, increasing steadily during the 2019 growing season, and peaking at  $0.84 \pm 0.25 \text{ mm}^3 \text{ l}^{-1}$  in September, despite water temperatures being higher in August (Figure S4 in Supporting Information S1). Freshwater cyanobacteria can produce CH<sub>4</sub> (Bižić et al., 2020), and high abundances of cyanobacteria have been linked to elevated lake CH<sub>4</sub> concentrations previously (Fazi et al., 2021), so this is a viable mechanism to explain growing season variations in surface water

CH<sub>4</sub>. However, Cyanobacteria biovolume also significantly correlated with chlorophyll *a* and TP (Figure S5 in Supporting Information S1), and it thus becomes difficult to decipher which variables are directly controlling CH<sub>4</sub> production, and which are correlated but not mechanistically related. If CH<sub>4</sub> is produced in surface waters (the importance of which is highly debated; Günthel et al., 2019; Peeters & Hofmann, 2021), rather than in sediments, then the apparent relationship with water depth (Figure 6g) could simply be due to shallow waters being closer to anthropogenic nutrient inputs (see Section 3.2).

### 3.4. Implications

Our measured CH<sub>4</sub> concentrations are in keeping with measurements from other large lakes, and we found a significant negative relationship between surface area of large lakes and average surface water CH<sub>4</sub> concentration ( $\rho = -0.46, p = 0.037$ ) (Table 1). This is in agreement with other studies that find inverse relationships between lake area and CH<sub>4</sub> emission (Holgerson & Raymond, 2016; Rosentreter et al., 2021). To generalize, these relationships might suggest that Lake Mälaren would be a minor source of diffusive CH<sub>4</sub> fluxes on a per area basis. However, it is important to consider that ebullition can be the dominant pathway for CH<sub>4</sub> release in some lakes (Bastviken et al., 2011; Sepulveda-Jauregui et al., 2015). In temperate lakes ebullition has mostly been observed to occur at depths <3–6 m (DelSontro et al., 2016; West et al., 2016). The far eastern basin in Mälaren has a mean depth of 3.4 m, and also has a relatively high nutrient concentration, and so ebullition may be large there. However, there is a lack of CH<sub>4</sub> ebullition measurements from very large lakes (Deemer & Holgerson, 2021) and so future studies of large lakes should prioritize this. Additionally, the spatiotemporal sampling design we used (11 stations sampled five times) could potentially underestimate CH<sub>4</sub> concentrations; recommendations based on data from three very small subarctic lakes are that diffusive emissions should be measured on at least 11 occasions, at three stations to minimize bias (Wik et al., 2016), although it is currently unknown how these findings might apply to large lakes such as Mälaren.

There is the chance that the synergistic effects of climate change and eutrophication could enhance GHG emissions from lakes (Meerhoff et al., 2022), and Mälaren is already showing signs of warming, with ice cover becoming less predictable in recent years (Knoll et al., 2019); indeed, our study year is unusual in being entirely ice-free. Ice-out CH<sub>4</sub> emissions can represent a sizable fraction of the annual budget (Jammet et al., 2015), but a shorter ice cover period can also lead to greater cumulative CH<sub>4</sub> emissions (Wik et al., 2014), and so the complete effect of rising temperatures on CH<sub>4</sub> dynamics in northern lakes is difficult to predict. As far as we are aware, our data represent the first published detailed surface water CH<sub>4</sub> measurements from any large lake within the European Union and thereby offer a snapshot through which to gauge future anthropogenic-induced changes in how large European lakes contribute to climatic warming.

### Acknowledgments

We thank Stina Drakare for her help in arranging the sampling, and for answering our many questions about Mälaren. We thank Gustav Pajala and David Bastviken for kindly allowing us to include their unpublished Vättern data in Table 1, and Joachim Audet, Yves Prairie, Antti J. Rissanen, and Bridget Deemer for pointing us to some studies for inclusion in Table 1 that we otherwise would have missed. We thank Mona Abbasi and Jeff Hawkes for interesting discussions about dissolved organic matter within Mälaren during the course of the project. We thank two anonymous reviewers and Bridget Deemer for their constructive review comments that helped to improve the manuscript, as well as the Associate Editor and Marguerite Xenopoulos (Editor in Chief) for their useful comments. Finally, we gratefully acknowledge the hard work and dedication of all those who collected and analyzed samples, and implemented and maintained the Mälaren monitoring program. No specific funding supported this work.

### Data Availability Statement

Methane data, and associated water chemistry and algal data, are available online as Peacock (2022), <https://doi.org/10.6084/m9.figshare.20026397.v4>. Additionally, all water chemistry and algae data are available online from the Swedish national monitoring program (Miljödata-MVM, 2022a) here: <https://miljodata.slu.se/MVM/Search>. Data from the 11 Mälaren sampling stations only can also be downloaded here (Miljödata-MVM, 2022b): <https://www.slu.se/en/departments/aquatic-sciences-assessment/research/forskningsprojekt/malaren-in-focus/environmental-assessment/>.

### References

- Bartoń, K. (2019). MuMIn: Multi-model inference. R package version 1.43.10. Retrieved from <https://CRAN.R-project.org/package=MuMIn>
- Bastviken, D., Cole, J., Pace, M., & Tranvik, L. (2004). Methane emissions from lakes: Dependence of lake characteristics, two regional assessments, and a global estimate. *Global Biogeochemical Cycles*, 18(4), GB4009. <https://doi.org/10.1029/2004GB002238>
- Bastviken, D., Tranvik, L. J., Downing, J. A., Crill, P. M., & Enrich-Prast, A. (2011). Freshwater methane emissions offset the continental carbon sink. *Science*, 331(6013), 50. <https://doi.org/10.1126/science.1196808>
- Bižić, M., Klintzsch, T., Ionescu, D., Hindiyeh, M. Y., Günthel, M., Muro-Pastor, A. M., et al. (2020). Aquatic and terrestrial cyanobacteria produce methane. *Science Advances*, 6(3), eaax5343. <https://doi.org/10.1126/sciadv.aax5343>
- Bogard, M. J., Del Giorgio, P. A., Boutet, L., Chaves, M. C. G., Prairie, Y. T., Merante, A., & Derry, A. M. (2014). Oxidic water column methanogenesis as a major component of aquatic CH<sub>4</sub> fluxes. *Nature Communications*, 5(1), 5350. <https://doi.org/10.1038/ncomms6350>
- Borges, A. V., Deirmendjian, L., Bouillon, S., Okello, W., Lambert, T., Roland, F. A., et al. (2022). Greenhouse gas emissions from African lakes are no longer a blind spot. *Science Advances*, 8(25), eabi8716. <https://doi.org/10.1126/sciadv.abi8716>

- Davidson, T. A., Audet, J., Jeppesen, E., Landkildehus, F., Lauridsen, T. L., Søndergaard, M., & Syväranta, J. (2018). Synergy between nutrients and warming enhances methane ebullition from experimental lakes. *Nature Climate Change*, 8(2), 156–160. <https://doi.org/10.1038/s41558-017-0063-z>
- Deemer, B. R., & Holgerson, M. A. (2021). Drivers of methane flux differ between lakes and reservoirs, complicating global upscaling efforts. *Journal of Geophysical Research: Biogeosciences*, 126(4), e2019JG005600. <https://doi.org/10.1029/2019jg005600>
- DelSontro, T., Beaulieu, J. J., & Downing, J. A. (2018). Greenhouse gas emissions from lakes and impoundments: Upscaling in the face of global change. *Limnology and Oceanography Letters*, 3(3), 64–75. <https://doi.org/10.1002/lol2.10073>
- DelSontro, T., Boutet, L., St-Pierre, A., del Giorgio, P. A., & Prairie, Y. T. (2016). Methane ebullition and diffusion from northern ponds and lakes regulated by the interaction between temperature and system productivity. *Limnology & Oceanography*, 61(S1), S62–S77. <https://doi.org/10.1002/lno.10335>
- Drakare, S., Wallman, K., Segersten, J., & Köhler, S. (2021). Fokus på Mälaren 2020: Sammanfattande resultat från miljöövervakning och forskningsprojekt knutna till samarbetet mellan SLU och Mälarens vattenvårdsförbund. *Rapport/Sveriges lantbruksuniversitet, Institutionen för vatten och miljö*, 10.
- Fazi, S., Amalfitano, S., Venturi, S., Pacini, N., Vazquez, E., Olaka, L. A., et al. (2021). High concentrations of dissolved biogenic methane associated with cyanobacterial blooms in East African lake surface water. *Communications Biology*, 4(1), 845. <https://doi.org/10.1038/s42003-021-02365-x>
- Fernandez, J. M., Townsend-Small, A., Zastepa, A., Watson, S. B., & Brandes, J. A. (2020). Methane and nitrous oxide measured throughout Lake Erie over all seasons indicate highest emissions from the eutrophic Western Basin. *Journal of Great Lakes Research*, 46(6), 1604–1614. <https://doi.org/10.1016/j.jglr.2020.09.011>
- Fink, G., Alcamo, J., Flörke, M., & Reeder, K. (2018). Phosphorus loadings to the world's largest lakes: Sources and trends. *Global Biogeochemical Cycles*, 32(4), 617–634. <https://doi.org/10.1002/2017gb005858>
- Gar'kusha, D. N., & Fedorov, Y. A. (2015). Distribution of methane concentration in coastal areas of the Gulf of Petrozavodsk, Lake Onega. *Water Resources*, 42(3), 331–339. <https://doi.org/10.1134/s0097807815030045>
- Graeber, D., Tenzin, Y., Stutter, M., Weigelhofer, G., Shatwell, T., von Tümpling, W., et al. (2021). Bioavailable DOC: Reactive nutrient ratios control heterotrophic nutrient assimilation—An experimental proof of the macronutrient-access hypothesis. *Biogeochemistry*, 155, 1–20. <https://doi.org/10.1007/s10533-021-00809-4>
- Grossart, H. P., Frindte, K., Dziallas, C., Eckert, W., & Tang, K. W. (2011). Microbial methane production in oxygenated water column of an oligotrophic lake. *Proceedings of the National Academy of Sciences of the United States of America*, 108(49), 19657–19661. <https://doi.org/10.1073/pnas.1110716108>
- Günthel, M., Donis, D., Kirillin, G., Ionescu, D., Bizic, M., McGinnis, D. F., et al. (2019). Contribution of oxic methane production to surface methane emission in lakes and its global importance. *Nature Communications*, 10(1), 5497. <https://doi.org/10.1038/s41467-019-13320-0>
- Herdendorf, C. E. (1982). Large lakes of the world. *Journal of Great Lakes Research*, 8(3), 379–412. [https://doi.org/10.1016/s0380-1330\(82\)71982-3](https://doi.org/10.1016/s0380-1330(82)71982-3)
- Hofmann, H., Federwisch, L., & Peeters, F. (2010). Wave-induced release of methane: Littoral zones as source of methane in lakes. *Limnology & Oceanography*, 55(5), 1990–2000. <https://doi.org/10.4319/lno.2010.55.5.1990>
- Holgerson, M. A., & Raymond, P. A. (2016). Large contribution to inland water CO<sub>2</sub> and CH<sub>4</sub> emissions from very small ponds. *Nature Geoscience*, 9(3), 222–226. <https://doi.org/10.1038/ngeo2654>
- IPCC. (2019). Refinement to the 2006 IPCC guidelines for national greenhouse gas inventories. In C. E. Lovelock, C. Evans, N. Barros, Y. Prairie, J. Alm, D. Bastviken, et al. (Eds.), *Agriculture, forestry and other land use (AFOLU). Chapter 7: Wetlands* (Vol. 4). Intergovernmental Panel on Climate Change.
- Jammet, M., Crill, P., Dengel, S., & Friborg, T. (2015). Large methane emissions from a subarctic lake during spring thaw: Mechanisms and landscape significance. *Journal of Geophysical Research: Biogeosciences*, 120(11), 2289–2305. <https://doi.org/10.1002/2015jg003137>
- Johansson, L., Temnerud, J., Abrahamsson, J., & Kleja, D. B. (2010). Variation in organic matter and water color in Lake Mälaren during the past 70 years. *Ambio*, 39(2), 116–125. <https://doi.org/10.1007/s13280-010-0019-2>
- Johnson, M. S., Matthews, E., Du, J., Genovese, V., & Bastviken, D. (2022). Methane emission from global lakes: New spatiotemporal data and observation-driven modeling of methane dynamics indicates lower emissions. *Journal of Geophysical Research: Biogeosciences*, 127(7), e2022JG006793. <https://doi.org/10.1029/2022jg006793>
- Joung, D., Leonte, M., & Kessler, J. D. (2019). Methane sources in the waters of Lake Michigan and Lake Superior as revealed by natural radiocarbon measurements. *Geophysical Research Letters*, 46(10), 5436–5444. <https://doi.org/10.1029/2019gl082531>
- Juutinen, S., Rantakari, M., Kortelainen, P., Huttunen, J. T., Larmola, T., Alm, J., et al. (2009). Methane dynamics in different boreal lake types. *Biogeosciences*, 6(2), 209–223. <https://doi.org/10.5194/bg-6-209-2009>
- Knoll, L. B., Sharma, S., Denfeld, B. A., Flaim, G., Hori, Y., Magnuson, J. J., et al. (2019). Consequences of lake and river ice loss on cultural ecosystem services. *Limnology and Oceanography Letters*, 4(5), 119–131. <https://doi.org/10.1002/lol2.10116>
- Laird, G. A., & Scavia, D. (1990). Distribution of labile dissolved organic carbon in Lake Michigan. *Limnology & Oceanography*, 35(2), 443–447. <https://doi.org/10.4319/lno.1990.35.2.0443>
- Lannergård, E. E., Fölster, J., & Futter, M. N. (2021). Turbidity-discharge hysteresis in a meso-scale catchment: The importance of intermediate scale events. *Hydrological Processes*, 35(12), 14435. <https://doi.org/10.1002/hyp.14435>
- Lannergård, E. E., Ledesma, J. L., Fölster, J., & Futter, M. N. (2019). An evaluation of high frequency turbidity as a proxy for riverine total phosphorus concentrations. *Science of the Total Environment*, 651, 103–113. <https://doi.org/10.1016/j.scitotenv.2018.09.127>
- Lauerwald, R., Allen, G. H., Deemer, B. R., Liu, S., Maavara, T., Raymond, P., et al. (2023a). Inland water greenhouse gas budgets for RECCAP2: 1. State-Of-The-Art of global scale assessments. *Global Biogeochemical Cycles*, 37(5), e2022GB007657. <https://doi.org/10.1029/2022gb007657>
- Lauerwald, R., Allen, G. H., Deemer, B. R., Liu, S., Maavara, T., Raymond, P., et al. (2023b). Inland water greenhouse gas budgets for RECCAP2: 2. Regionalization and homogenization of estimates. *Global Biogeochemical Cycles*, 37(5), e2022GB007658. <https://doi.org/10.1029/2022gb007658>
- Ledesma, J. L., Köhler, S. J., & Futter, M. N. (2012). Long-term dynamics of dissolved organic carbon: Implications for drinking water supply. *Science of the Total Environment*, 432, 1–11. <https://doi.org/10.1016/j.scitotenv.2012.05.071>
- Li, L., Xue, B., Yao, S., Tao, Y., & Yan, R. (2018). Spatial-temporal patterns of methane dynamics in Lake Taihu. *Hydrobiologia*, 822(1), 143–156. <https://doi.org/10.1007/s10750-018-3670-4>
- Li, M., Peng, C., Zhu, Q., Zhou, X., Yang, G., Song, X., & Zhang, K. (2020a). The significant contribution of lake depth in regulating global lake diffusive methane emissions. *Water Research*, 172, 115465. <https://doi.org/10.1016/j.watres.2020.115465>
- Li, Z., Lu, L., Lv, P., Zhang, Z., & Guo, J. (2020b). Imbalanced stoichiometric reservoir sedimentation regulates methane accumulation in China's Three Gorges Reservoir. *Water Resources Research*, 56(9), 2019WR026447. <https://doi.org/10.1029/2019wr026447>

- Liu, L., Xu, M., Li, R., & Shao, R. (2017). Timescale dependence of environmental controls on methane efflux from Poyang Hu, China. *Biogeosciences*, 14(8), 2019–2032. <https://doi.org/10.5194/bg-14-2019-2017>
- Mandryk, R. R., Capelle, D. W., Manning, C. C., Tortell, P., McCulloch, R. D., & Papakyriakou, T. (2021). First estimation of the diffusive methane flux and concentrations from Lake Winnipeg, a large, shallow and eutrophic lake. *Journal of Great Lakes Research*, 47(3), 741–750. <https://doi.org/10.1016/j.jglr.2021.03.011>
- Meerhoff, M., Audet, J., Davidson, T. A., De Meester, L., Hilt, S., Kosten, S., et al. (2022). Feedback between climate change and eutrophication: Revisiting the allied attack concept and how to strike back. *Inland Waters*, 12(2), 1–18. <https://doi.org/10.1080/20442041.2022.2029317>
- Miljödata-MVM. (2022a). National data host lakes and watercourses, and national data host agricultural land [Dataset]. Swedish University of Agricultural Sciences (SLU). Retrieved from <https://miljodata.slu.se/mvm/>
- Miljödata-MVM. (2022b). National data host lakes and watercourses, and national data host agricultural land [Dataset]. Swedish University of Agricultural Sciences (SLU). Retrieved from <https://www.slu.se/en/departments/aquatic-sciences-assessment/research/forskningsprojekt/malaren-in-focus/environmental-assessment/>
- Minor, E. C., & Oyler, A. R. (2021). Dissolved organic matter in large lakes: A key but understudied component of the carbon cycle. *Biogeochemistry*, 164(1), 295–318. <https://doi.org/10.1007/s10533-020-00733-z>
- Miyajima, T., Yamada, Y., Wada, E., Nakajima, T., Koitabashi, T., Hanba, Y. T., & Yoshii, K. (1997). Distribution of greenhouse gases, nitrite, and  $\delta^{13}\text{C}$  of dissolved inorganic carbon in Lake Biwa: Implications for hypolimnetic metabolism. *Biogeochemistry*, 36(2), 205–221. <https://doi.org/10.1023/a:1005702707183>
- Nakagawa, S., & Schielzeth, H. (2013). A general and simple method for obtaining R<sup>2</sup> from generalized linear mixed-effects models. *Methods in Ecology and Evolution*, 4(2), 133–142. <https://doi.org/10.1111/j.2041-210x.2012.00261.x>
- Natchimuthu, S., Sundgren, I., Gålfalk, M., Klemmedtsson, L., Crill, P., Danielsson, Å., & Bastviken, D. (2016). Spatio-temporal variability of lake CH<sub>4</sub> fluxes and its influence on annual whole lake emission estimates. *Limnology & Oceanography*, 61(S1), S13–S26. <https://doi.org/10.1002/lno.10222>
- Peacock, M. (2022). Mälaren methane concentrations [Dataset]. figshare. <https://doi.org/10.6084/m9.figshare.20026397.v4>
- Peacock, M., Futter, M. N., Jutterström, S., Kothawala, D. N., Moldan, F., Stadmark, J., & Evans, C. D. (2022). Three decades of changing nutrient stoichiometry from source to sea on the Swedish west coast. *Ecosystems*, 25(8), 1–16. <https://doi.org/10.1007/s10021-022-00798-x>
- Peacock, M., Ridley, L. M., Evans, C. D., & Gauci, V. (2017). Management effects on greenhouse gas dynamics in fen ditches. *Science of the Total Environment*, 578, 601–612. <https://doi.org/10.1016/j.scitotenv.2016.11.005>
- Peeters, F., & Hofmann, H. (2021). Oxidic methanogenesis is only a minor source of lake-wide diffusive CH<sub>4</sub> emissions from lakes. *Nature Communications*, 12(1), 1206. <https://doi.org/10.1038/s41467-021-21215-2>
- Pinheiro, J., Bates, D., DebRoy, S., & Sarkar, D., & R Core Team. (2018). nlme: Linear and nonlinear mixed effects models. R package version 3.1-137. Retrieved from <https://CRAN.R-project.org/package=nlme>
- Prairie, Y. T., Alm, J., Beaulieu, J., Barros, N., Battin, T., Cole, J., et al. (2018). Greenhouse gas emissions from freshwater reservoirs: What does the atmosphere see? *Ecosystems*, 21(5), 1058–1071. <https://doi.org/10.1007/s10021-017-0198-9>
- R Core Team. (2013). *R: A language and environment for statistical computing*. R Foundation for Statistical Computing. Retrieved from <http://www.R-project.org/>
- Reddy, K. R., Fisher, M. M., & Ivanoff, D. (1996). Resuspension and diffusive flux of nitrogen and phosphorus in a hypereutrophic lake. *American Society of Agronomy, Crop Science Society of America, and Soil Science Society of America*, 25(2), 363–371. <https://doi.org/10.2134/jeq1996.00472425002500020022x>
- Rehrl, A. L., Golovko, O., Ahrens, L., & Köhler, S. (2020). Spatial and seasonal trends of organic micropollutants in Sweden's most important drinking water reservoir. *Chemosphere*, 249, 126168. <https://doi.org/10.1016/j.chemosphere.2020.126168>
- Roberts, H. M., & Shiller, A. M. (2015). Determination of dissolved methane in natural waters using headspace analysis with cavity ring-down spectroscopy. *Analytica Chimica Acta*, 856, 68–73. <https://doi.org/10.1016/j.aca.2014.10.058>
- Roland, F. A., Morana, C., Darchambeau, F., Crowe, S. A., Thamdrup, B., Descy, J. P., & Borges, A. V. (2018). Anaerobic methane oxidation and aerobic methane production in an east African great lake (Lake Kivu). *Journal of Great Lakes Research*, 44(6), 1183–1193. <https://doi.org/10.1016/j.jglr.2018.04.003>
- Rosentreter, J. A., Borges, A. V., Deemer, B. R., Holgerson, M. A., Liu, S., Song, C., et al. (2021). Half of global methane emissions come from highly variable aquatic ecosystem sources. *Nature Geoscience*, 14(4), 225–230. <https://doi.org/10.1038/s41561-021-00715-2>
- Saunio, M., Stavert, A. R., Poulter, B., Bousquet, P., Canadell, J. G., Jackson, R. B., et al. (2020). The global methane budget 2000–2017. *Earth System Science Data*, 12(3), 1561–1623. <https://doi.org/10.5194/essd-12-1561-2020>
- Schmid, M., Batist, M. D., Granin, N. G., Kapitanov, V. A., McGinnis, D. F., Mizandrontsev, I. B., et al. (2007). Sources and sinks of methane in Lake Baikal: A synthesis of measurements and modeling. *Limnology & Oceanography*, 52(5), 1824–1837. <https://doi.org/10.4319/lo.2007.52.5.1824>
- Schulz, S., Matsuyama, H., & Conrad, R. (1997). Temperature dependence of methane production from different precursors in a profundal sediment (Lake Constance). *FEMS Microbiology Ecology*, 22(3), 207–213. <https://doi.org/10.1111/j.1574-6941.1997.tb00372.x>
- Segers, R. (1998). Methane production and methane consumption: A review of processes underlying wetland methane fluxes. *Biogeochemistry*, 41(1), 23–51.
- Sepulveda-Jauregui, A., Walter Anthony, K. M., Martínez-Cruz, K., Greene, S., & Thalasso, F. (2015). Methane and carbon dioxide emissions from 40 lakes along a north–south latitudinal transect in Alaska. *Biogeosciences*, 12(11), 3197–3223. <https://doi.org/10.5194/bg-12-3197-2015>
- Sjors, H. (1999). The background: Geology, climate and zonation. *Acta Phytogeographica Suecica*, 84, 5–14.
- SLU. (2022). Geochemical laboratory, accredited analytical methods. Retrieved from <https://www.slu.se/en/departments/aquatic-sciences-assessment/laboratories/vattenlab2/>
- SMHI. (2022a). Damm-och sjöregister. Mälaren, sjöidentitet 658080-162871. Retrieved from <https://vattenwebb.smhi.se/svarwebb/>
- SMHI. (2022c). Meteorologi. Adelsö A, stationsnummer 97280. Retrieved from <https://www.smhi.se/data/meteorologi/>
- SMHI. (2022b). Modelldata per område. Delavrinningsområdets namn: Utloppet av Mälaren. Retrieved from <https://vattenwebb.smhi.se/modelarea/>
- SMHI. (2022d). Statistik islägning och islossning. Is på sjöar och vattendrag. Retrieved from <https://www.smhi.se/data/hydrologi/is-pa-sjoar-och-vattendrag>
- Soares, A. R., Lapiere, J. F., Selvam, B. P., Lindström, G., & Berggren, M. (2019). Controls on dissolved organic carbon bioreactivity in river systems. *Scientific Reports*, 9(1), 14897. <https://doi.org/10.1038/s41598-019-50552-y>
- Sollberger, S., Corella, J. P., Girardclos, S., Randlett, M. E., Schubert, C. J., Senn, D. B., et al. (2014). Spatial heterogeneity of benthic methane dynamics in the subaquatic canyons of the Rhone River Delta (Lake Geneva). *Aquatic Sciences*, 76(S1), 89–101. <https://doi.org/10.1007/s00027-013-0319-2>

- Sonesten, L., Wallman, K., Axenrot, T., Beier, U., Drakare, S., Ecke, F., et al. (2013). *Mälaren Tillståndsutvecklingen 1965–2011*. (Vol. 1). Sveriges lantbruksuniversitet (SLU), Institutionen för vatten och miljö. Rapport. ISBN: 978-91-576-9139-2. <https://pub.epsilon.slu.se/11297/>
- Sturm, K., Keller-Lehmann, B., Werner, U., Raj Sharma, K., Grinham, A. R., & Yuan, Z. (2015). Sampling considerations and assessment of E xetainer usage for measuring dissolved and gaseous methane and nitrous oxide in aquatic systems. *Limnology and Oceanography: Methods*, *13*(7), 375–390. <https://doi.org/10.1002/lom3.10031>
- Stutter, M. I., Graeber, D., Evans, C. D., Wade, A. J., & Withers, P. J. A. (2018). Balancing macronutrient stoichiometry to alleviate eutrophication. *Science of the Total Environment*, *634*, 439–447. <https://doi.org/10.1016/j.scitotenv.2018.03.298>
- Taylor, P. G., & Townsend, A. R. (2010). Stoichiometric control of organic carbon–nitrate relationships from soils to the sea. *Nature*, *464*(7292), 1178–1181. <https://doi.org/10.1038/nature08985>
- Tong, Y., Zhang, W., Wang, X., Couture, R. M., Larssen, T., Zhao, Y., et al. (2017). Decline in Chinese lake phosphorus concentration accompanied by shift in sources since 2006. *Nature Geoscience*, *10*(7), 507–511. <https://doi.org/10.1038/ngeo2967>
- Wang, H., Huang, R., Li, J., Chen, Q., & Ma, T. (2021). Dissolved and emitted methane in the Poyang Lake. *Science China Technological Sciences*, *64*(1), p203–212. <https://doi.org/10.1007/s11431-020-1594-6>
- Webb, J. R., Clough, T. J., & Quayle, W. C. (2021). A review of indirect N<sub>2</sub>O emission factors from artificial agricultural waters. *Environmental Research Letters*, *16*(4), 043005. <https://doi.org/10.1088/1748-9326/abed00>
- Weishaar, J. L., Aiken, G. R., Bergamaschi, B. A., Fram, M. S., Fujii, R., & Mopper, K. (2003). Evaluation of specific ultraviolet absorbance as an indicator of the chemical composition and reactivity of dissolved organic carbon. *Environmental Science & Technology*, *37*(20), 4702–4708. <https://doi.org/10.1021/es030360x>
- West, W. E., Creamer, K. P., & Jones, S. E. (2016). Productivity and depth regulate lake contributions to atmospheric methane. *Limnology & Oceanography*, *61*(S1), S51–S61. <https://doi.org/10.1002/lno.10247>
- Wiesenburg, D. A., & Guinasso, N. L., Jr. (1979). Equilibrium solubilities of methane, carbon monoxide, and hydrogen in water and sea water. *Journal of Chemical and Engineering Data*, *24*(4), 356–360. <https://doi.org/10.1021/jc60083a006>
- Wik, M., Thornton, B. F., Bastviken, D., MacIntyre, S., Varner, R. K., & Crill, P. M. (2014). Energy input is primary controller of methane bubbling in subarctic lakes. *Geophysical Research Letters*, *41*(2), 555–560. <https://doi.org/10.1002/2013gl058510>
- Wik, M., Thornton, B. F., Bastviken, D., Uhlbäck, J., & Crill, P. M. (2016). Biased sampling of methane release from northern lakes: A problem for extrapolation. *Geophysical Research Letters*, *43*(3), 1256–1262. <https://doi.org/10.1002/2015gl066501>
- Wilkinson, J., Bors, C., Burgis, F., Lorke, A., & Bodmer, P. (2018). Measuring CO<sub>2</sub> and CH<sub>4</sub> with a portable gas analyzer: Closed-loop operation, optimization and assessment. *PLoS One*, *13*(4), e0193973. <https://doi.org/10.1371/journal.pone.0193973>
- Yvon-Durocher, G., Allen, A. P., Bastviken, D., Conrad, R., Gudas, C., St-Pierre, A., et al. (2014). Methane fluxes show consistent temperature dependence across microbial to ecosystem scales. *Nature*, *507*(7493), 488–491. <https://doi.org/10.1038/nature13164>
- Zheng, Y., Wu, S., Xiao, S., Yu, K., Fang, X., Xia, L., et al. (2022). Global methane and nitrous oxide emissions from inland waters and estuaries. *Global Change Biology*, *28*(15), 4713–4725. <https://doi.org/10.1111/gcb.16233>
- Zhou, Z., Guo, L., & Minor, E. C. (2016). Characterization of bulk and chromophoric dissolved organic matter in the Laurentian Great Lakes during summer 2013. *Journal of Great Lakes Research*, *42*(4), 789–801. <https://doi.org/10.1016/j.jglr.2016.04.006>